Highly thermosensitive Ca^{2+} dynamics in a HeLa cell through IP_3 receptors

Vadim Tseeb,[1,2] Madoka Suzuki,[3] Kotaro Oyama,[1] Kaoru Iwai,[4] and Shin'ichi Ishiwata[1,3]

[1]Department of Physics, Faculty of Science and Engineering, Waseda University, 3-4-1 Okubo, Shinjuku-ku, Tokyo 169-8555, Japan
[2]Institute of Theoretical and Experimental Biophysics, Russian Academy of Sciences, Pushchino, Moscow Region 142290, Russia
[3]Consolidated Research Institute for Advanced Science and Medical Care, Waseda University, 513 Wasedatsurumaki-cho, Shinjuku-ku, Tokyo 162-0041, Japan
[4]Department of Chemistry, Faculty of Science, Nara Women's University, Kitauoya-Nishimachi, Nara 630-8506, Japan

(Received 21 October 2008; accepted 1 January 2009; published online 4 March 2009)

Intracellular Ca^{2+} distribution and its dynamics are essential for various cellular functions. We show with single HeLa cells that a microscopic heat pulse induces Ca^{2+} uptake into intracellular stores during heating and Ca^{2+} release from them at the onset of recooling, and the overshoot of Ca^{2+} release occurs above the critical value of a temperature change, which decreases from 1.5 to 0.2 °C on increasing the experimental temperature from 22 to 37 °C. This highly thermosensitive Ca^{2+} dynamics is probably attributable to the altered balance between Ca^{2+} uptake by endoplasmic reticulum Ca^{2+}-ATPases and Ca^{2+} release via inositol 1,4,5-trisphosphate receptors. These results suggest that Ca^{2+} signaling is extremely sensitive to temperature changes, especially around body temperature, in cells expressing inositol 1,4,5-trisphosphate receptors.
[DOI: 10.2976/1.3073779]

CORRESPONDENCE
Shin'ichi Ishiwata:
ishiwata@waseda.jp

Temperature is an essential parameter that determines physical and chemical processes in the homeostasis of living cells. A temperature change shifts the electrochemical equilibrium of ions (Cantor and Schimmel, 1980), and a temperature gradient generates the directional motion of particles (Duhr and Braun, 2006). Therefore, the induction of temperature change confined within the microvolume inside a cell will provide a new dimension not only to nanotechnology (Hamann *et al.*, 2006), but also to cellular thermophysiology and the treatment of tumors (Hirsch *et al.*, 2003; Kam *et al.*, 2005; Pissuwan *et al.*, 2006).

Biological systems are temperature-sensitive at various levels of hierarchy, from single molecules to cells, tissues, and organisms. For example, fertilization in mammals is navigated by the temperature gradient (Bahat *et al.*, 2003); an increase in neuronal activity associated with temperature elevations has been observed in the hippocampus (Andersen and Moser, 1995); sex in reptiles is determined by the absolute temperature (Warner and Shine, 2008); and plants react to temperature stresses to maximize growth and developmental processes (Sung *et al.*, 2003). It has recently been clarified that ambient thermoreceptors are expressed as a family of channels in the specific regions in the brain (Hamada *et al.*, 2008), sensory nerve endings, and skin (Dhaka *et al.*, 2006). The temperature in cells, however, has been frequently treated as a nonlocal macroscopic parameter of the huge environment surrounding the cell, thereby as being constant or slowly changing. One reason for this treatment is the belief that, because of the fast thermal diffusion in aqueous media, the temperature within a cell is kept uniform even when heat production occurs locally. In addition, only a few experimental methods have been developed to apply a local heat pulse and measure temperature at the single-cell level. Therefore, although it is theoretically possible to define

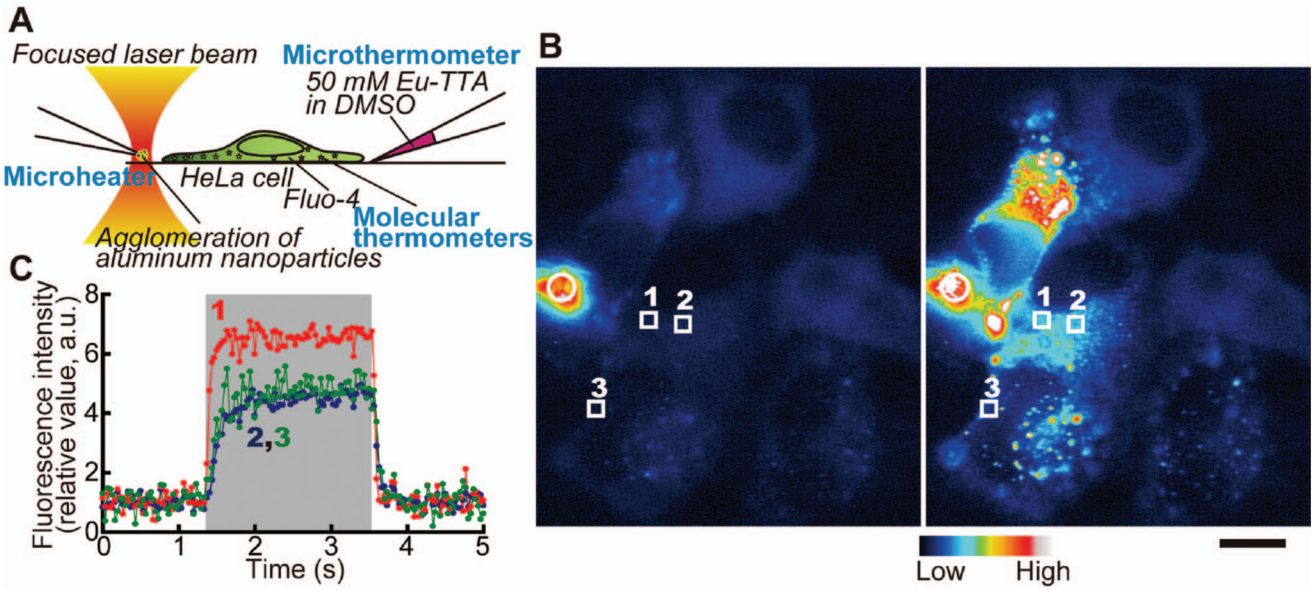

Figure 1. Experimental setup and the temperature change inside cells. (A) Illustration of the setup. (B) Fluorescence images before (left) and during (right) heat pulse. Nuclei looked dark as the fluorescent thermosensitive polymers were injected into the cytoplasm. White rectangles with numbers represent the regions of interest (ROIs) analyzed in (C). White circles indicate the position of the microheater. Scale bar: 10 μm. Each image, which is an average of 30 video frames, is shown in pseudocolors. Brightness and contrast were artificially enhanced for display purposes. (C) Time course of the fluorescence intensity of the fluorescent thermosensitive polymers in the ROIs indicated in (B). In each ROI, background level was subtracted (for raw data, see Supplementary Materials, Fig. S1). Then the relative fluorescence intensity was obtained against the average between 0 and 1 s just before a heat pulse. Each dot shows the value in a single video frame (33 ms). Numbers represent the ROIs analyzed. The large gray column shows the time during which the microheater was illuminated by the laser beam. The microheater allowed us to easily create a reversible temperature gradient while keeping the base temperature constant.

local temperature down to the submicrometer level in water (Kondepudi and Prigogine, 1998), to the best of our knowledge, no studies have applied heat pulse to single eukaryotic cells and observed their responses, to understand temperature-dependent processes [for prokaryotic cells, i.e., *Escherichia coli*, see Maeda *et al.* (Maeda *et al.*, 1976) and Paster and Ryu (Paster and Ryu, 2008)].

Thus, we exposed HeLa cells to heat pulses and observed changes in cytoplasmic free Ca^{2+} concentration ($[Ca^{2+}]_{cyt}$), which controls most cellular processes (Berridge *et al.*, 1998). Our results show that the intracellular $[Ca^{2+}]$ can be modulated by subtle temperature changes on the order of a few tenths degrees centigrade, especially around the body temperature. We demonstrate that the channels involved in this process are the widely expressed IP_3 receptors.

RESULTS AND DISCUSSION

Production of heat pulse and measurement of quick temperature changes in the cytoplasm

Microscopic heat pulse (rectangular temperature change) was produced by an infrared laser beam focused on an agglomeration of metal nanoparticles at the tip of a glass micropipette placed near single living HeLa cells, such that the local temperature gradient within several tens of micrometers was created in solution (Kato *et al.*, 1999; Zeeb *et al.*, 2004) [Fig. 1(A)].

We first examined the rates of temperature increase and decrease in the cytoplasm using fluorescent thermosensitive polymers (Uchiyama *et al.*, 2004) as molecular thermometers, the fluorescence intensity of which abruptly increases about 15-fold when the temperature is elevated from 20 to 27 °C. For these measurements, molecular thermometers were injected into the cytoplasm (Fig. 1 and Supplementary Materials, Fig. S1). We found that the temperature of the cytoplasm rose and fell as much as several degrees centigrade within 300 and 100 ms [Figs. 1(B) and 1(C)], respectively.

Ca^{2+} dynamics in HeLa cells induced by heat pulses

When cells were exposed to heat pulse, the fluorescence intensity of Fluo-4, i.e., $[Ca^{2+}]_{cyt}$, initially decreased upon heating (Fig. 2). This response could be clearly distinguished from the photobleaching process, the change of the intrinsic temperature-related properties of Fluo-4 such as thermal quenching, or the elevated background level caused by laser diffraction. Then, at the onset of recooling, the fluorescence intensity of Fluo-4 noticeably increased, indicating a transient increase in $[Ca^{2+}]_{cyt}$. This overshoot of Ca^{2+} release was

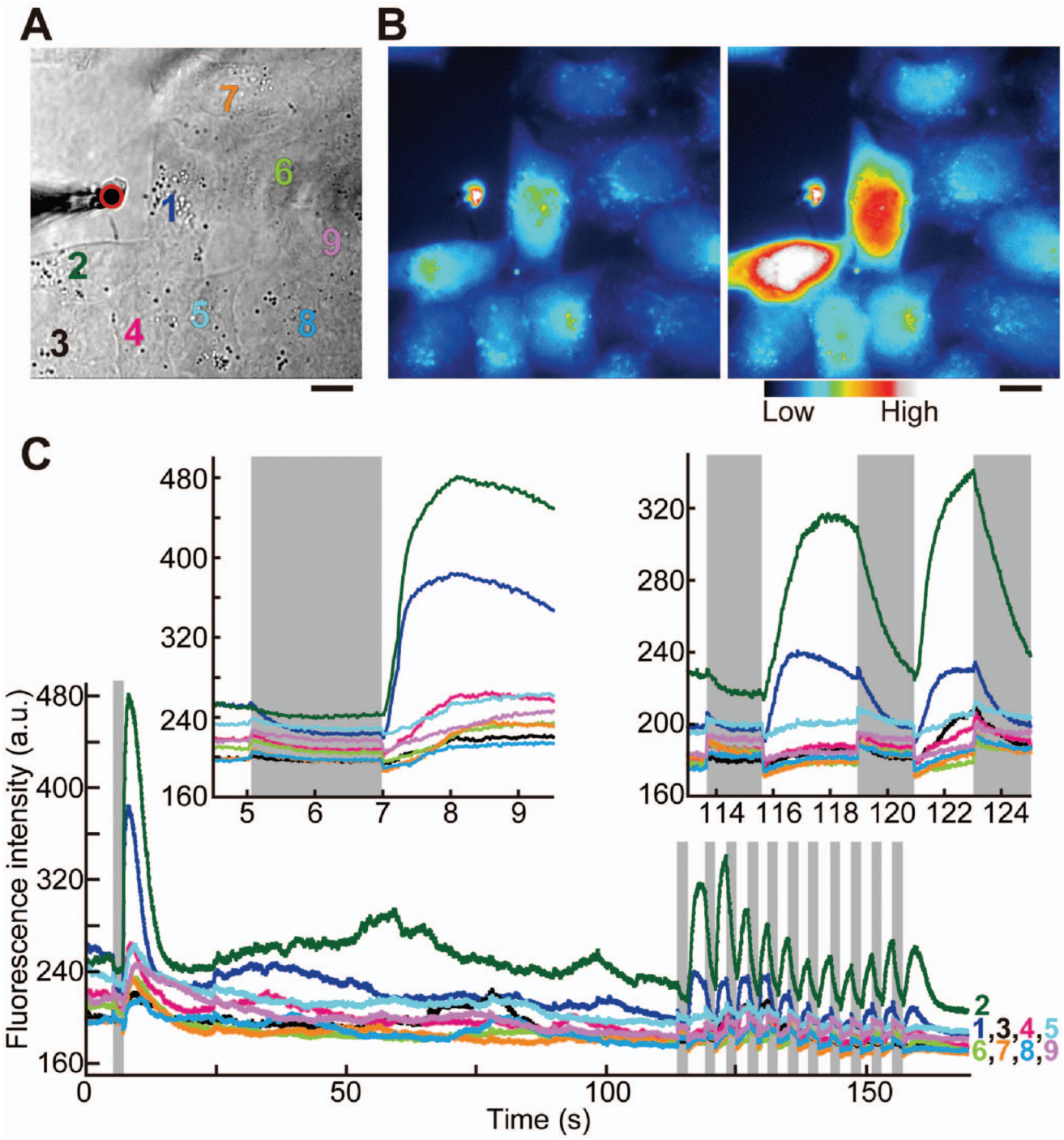

Figure 2. Ca^{2+} response of cells to heat pulses at 37 °C. (A) Bright field image of cells and a microheater. Colored numbers represent cells analyzed. The red circle represents the position of the microheater. (B) Fluorescence image of Fluo-4. Left and right images, which are averages of those obtained between 3–4.5 s (45 frames) and 7.5–9 s (45 frames) in (C), respectively, are shown in pseudocolors. Scale bar: 10 μm. Brightness and contrast of images in (A) and (B) were artificially enhanced for display purposes. (C) Time courses of the fluorescence intensity of Fluo-4 for each cell. Cells were exposed to heat pulses with amplitudes of about 0.5–2.0 °C. The two insets show magnified views of two parts of (C). (The insets are also presented as Supplementary Materials, Videos 1 and 2, respectively.) Gray columns show the times during which the microheater was illuminated by the laser beam.

often followed by $[Ca^{2+}]_{cyt}$ oscillations, but in all cases the fluorescence intensity eventually returned to its initial level (see also Supplementary Materials, Video 1). When short heat pulses were repeatedly applied [11 times in Fig. 2(C)], cells responded in the same manner [Fig. 2 (inset), and Supplementary Materials, Video 2]. The convection of the water flow was not the cause of Ca^{2+} overshoot, because at such weak and short heat pulses as used here, the convection was localized near the heat source (Supplementary Materials, Videos 3–5).

Identification of Ca^{2+} source and Ca^{2+}-release channels

Which component(s) in the cell is (are) responsible? First, we examined the source of Ca^{2+}. When the same experiment was performed in the absence of extracellular Ca^{2+} (Supplementary Materials, Fig. S2), $[Ca^{2+}]_{cyt}$ decreased during heating, followed by a Ca^{2+} overshoot upon recooling. However, the amplitude of the Ca^{2+} overshoot decreased for successive pulses. These observations point to the intracellular Ca^{2+} stores as an origin of Ca^{2+} overshoot. The cells located farther from the heat source predictably started to respond later than the cells located closer to it. This indicates that Ca^{2+} stores in more distant cells need more heat pulses to accumulate sufficient amount of Ca^{2+} to induce Ca^{2+} overshoot. When the cells were treated with thapsigargin, an inhibitor of the sarco/endoplasmic reticulum Ca^{2+}-ATPase (SERCA), it produced a continuous leak of Ca^{2+} from endoplasmic reticulum (ER), and the cells became absolutely insensitive to heat pulses (Supplementary Materials, Fig. S3). Therefore, the ER is probably the most important store of Ca^{2+} involved in the thermosensitive Ca^{2+} dynamics. For the refilling of Ca^{2+} in ER, the store-operated Ca^{2+} entry (SOCE) channels may be responsible.

Next, we determined the Ca^{2+}-release channel responsible for this thermosensitivity. The response of ryanodine receptors (RyRs) in muscle to cooling from room temperature to ~5 °C in a few seconds is known as rapid cooling (RC) and has been extensively studied (Bers, 1989; Protasi *et al.*, 2004; Sakai, 1986). Others have suggested that the mechanism of the rapid cooling contracture (RCC) by which RC causes a contracture in a muscle fiber treated with caffeine is partially caused by inositol 1,4,5-trisphosphate receptors (IP_3Rs) (Talon *et al.*, 2000). However, no study has examined the response to small temperature changes as used here. Since a HeLa cell is known to express a small amount of RyRs (Bennett *et al.*, 1996) in addition to a large amount of IP_3Rs, we tested if a Ca^{2+} overshoot occurred when the function of RyRs was inhibited (Ehrlich *et al.*, 1994; Meissner, 1986). We found that the cells responded even in the presence of 100 μM ryanodine, an inhibitor of RyRs (Supplementary Materials, Fig. S4). Next, we examined the effect of heparin, known both as an inhibitor of IP_3Rs and as an activator of RyRs (Ehrlich *et al.*, 1994). No Ca^{2+} overshoot was observed (Supplementary Materials, Fig. S5 and Table S1), indicating that the involved Ca^{2+}-release channels are not the RyRs, but the IP_3Rs. In these measurements, the largest amplitude of Ca^{2+} overshoot was comparable to the amplitude of the response induced by an addition of 100 μM histamine, which releases Ca^{2+} from ER through IP_3R. Therefore, it also indicates that heat pulse can be used as a new powerful method to manipulate intracellular Ca^{2+} [e.g., to produce a triangular Ca^{2+} wave, as shown in Fig. 2 and Supplementary Materials, Figs. S4(C) and S4(E)].

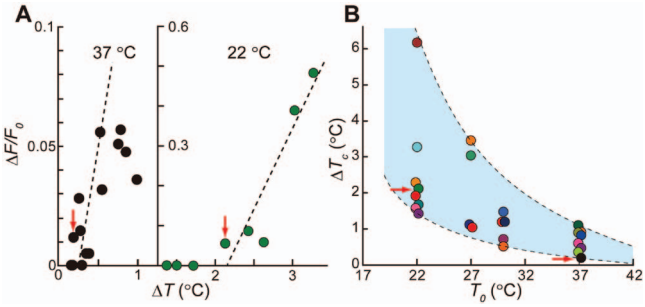

Figure 3. Correlation of base temperature (T_0) with the critical value of the amplitude of temperature change (ΔT) to induce Ca^{2+} overshoot (ΔT_c). (A) Typical examples of $\Delta F/F_0$ plotted against various ΔT in the same preparation at 37 °C (left) and 22 °C (right). $\Delta F/F_0$ is defined in Materials and Methods. The left and the right sides of (A) are derived from Supplementary Material Figs. S6(A) and S6(D), left, respectively. The dashed lines are a linear fit for the data at $\Delta F/F_0 > 0$. Red arrows show the most sensitive cell in each measurement (ΔT_c). (B) Effect of T_0 on the ΔT_c distribution. Each ΔT_c represented by a color symbol was determined from the data in Supplementary Materials, Fig. S6. All cells responded to temperature changes with ΔT over the upper border of the light blue area. None of cells responded to temperature changes with ΔT below the lower border. Red arrows indicate the same data points as in (A).

Cellular response depends on both the amplitude of the temperature change and the base temperature

The amplitude of the temperature change (ΔT) in a cell depends on the distance from the heat source. In this study, we measured the temperature field profiles around the microheater using a microthermometer (Zeeb *et al.*, 2004) after each experiment [Fig. 1(A) and Supplementary Materials, Videos 3–5]. ΔT of a cell was determined from the temperature field profile at the position of the nucleus. By plotting the maximum amplitude of Ca^{2+} overshoot upon recooling, i.e., $\Delta F/F_0$, against ΔT [Figs. 3(A) and Supplementary Materials, Fig. S6], we found that a larger ΔT induced a stronger Ca^{2+} overshoot. In addition, there was a critical value of ΔT (ΔT_c), i.e., the minimal ΔT required for the occurrence of a Ca^{2+} overshoot [red arrows in Fig. 3(A)]. To test the effect of the base temperature (T_0), the same experiments were performed at 30, 27, and 22 °C, and a similar change in $[Ca^{2+}]_{cyt}$ was observed (Supplementary Materials, Fig. S7). Furthermore, at each T_0, $\Delta F/F_0$ increased with an

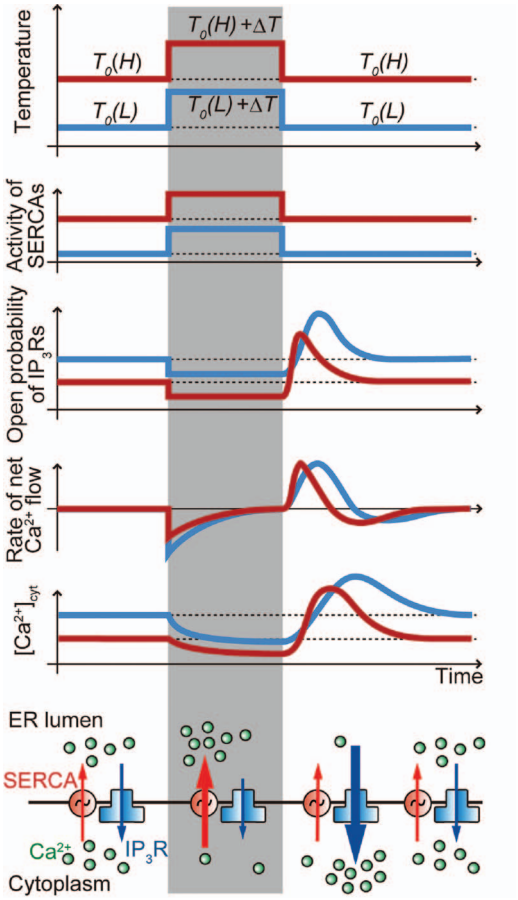

Figure 4. Schematic of the response of various cellular parameters to heat pulse. Application of rectangular temperature change alters the balance between the Ca^{2+} outflux from the cytoplasm regulated by SERCAs and the Ca^{2+} influx determined by IP_3Rs, resulting in Ca^{2+} overshoot at the onset of recooling. The time course of $[Ca^{2+}]_{cyt}$ (the fifth diagram from the top) is created by the integral of the rate of net Ca^{2+} flow (the fourth diagram from the top). Gray columns show the times during which the microheater was illuminated by the laser beam. All the quantities on the ordinates are represented by an arbitrary unit. Red and blue lines show the states at higher $[T_0(H)]$ and lower $[T_0(L)]$ base temperatures, respectively.

increase in ΔT, while ΔT_c diminishes with increasing T_0 (Fig. 3 and Supplementary Materials, Fig. S6). In the most sensitive cells ΔT_c was 1.5 °C at 22 °C and 0.2 °C at 37 °C [Fig. 3(B)]. The T_0-dependent ΔT_c was broadly distributed [the light blue area of Fig. 3(B)], suggesting the existence of a wide variety of the internal states of cells (e.g., the Ca^{2+} distribution in the cytoplasm and ER lumen).

Mechanism of observed Ca^{2+} dynamics

Based on the above results and previous reports concerning SERCA and Ca^{2+} release channel, we suggest a mechanism for the highly sensitive Ca^{2+} uptake and release associated with a heat pulse (Fig. 4). Prior to a heat pulse, the pumping activity of SERCAs and the leak of Ca^{2+} through the IP_3Rs are balanced (the raw data are shown in Supplementary Materials, Fig. S8). Upon the application of a heat pulse, SERCA activity is promoted, and at the same time the open probability of IP_3Rs decreases similarly to the RyRs (Protasi *et al.*, 2004; Sitsapesan *et al.*, 1991). These changes shift the net Ca^{2+} flow toward the filling of ER. This Ca^{2+} flow continues until the new steady state with the larger gradient of $[Ca^{2+}]$ between the cytoplasm and ER lumen is reached.

How does the Ca^{2+} overshoot occur? In the studies of RCC (Protasi *et al.*, 2004; Sitsapesan *et al.*, 1991) it has been proposed that RC transiently increases the open probability of RyRs. Our findings suggest that IP_3Rs have a similar property; at the same time, the pumping activity of SERCA quickly returns to the level prior to heat pulse. This alters the delicate balance between the activities of SERCA and IP_3R. Larger ΔT creates a steeper $[Ca^{2+}]$ gradient, which leads to a larger Ca^{2+} overshoot. In addition, a higher T_0 causes a larger $[Ca^{2+}]$ gradient at the steady state, resulting in a stronger Ca^{2+} overshoot at smaller ΔT. Previous studies have shown that both an amplitude of $[Ca^{2+}]_{cyt}$ increase in plant cells (Plieth *et al.*, 1999) and paramecium (Inoue and Nakaoka, 1990) and the initial tension rise in skeletal muscle upon RCC (Sakai, 1986) depend linearly on the applied rate of RC. Although the channels operating in these cells may be different, both conclusions correlate.

Using the heat pulse method, we found a new link between temperature and Ca^{2+} dynamics. Recent studies on the mechanism of biological temperature-sensing have identified various kinds of thermoreceptors located in, for example, skin, sensory endings, and brain (Dhaka *et al.*, 2006; Hamada *et al.*, 2008; Patapoutian *et al.*, 2003). In this study we characterized a new type of thermosensitivity, which is based on the asymmetrical thermosensitive response of the Ca^{2+} uptake by SERCAs and its outflow via IP_3Rs. This mechanism allows cells to respond very sensitively (by changing $[Ca^{2+}]_{cyt}$) to temperature changes.

Our results suggest that the transient temperature change can modulate Ca^{2+} dynamics, and ΔT_c reaches zero as T_0 approaches 42 °C, which is a fatal body temperature for humans. Normal body temperature (~37 °C) is set just below the fatal temperature but remains within the region of high thermosensitivity. Because IP_3Rs are abundantly expressed in most types of cells (Mikoshiba, 2007), this is possibly a general mechanism underlying temperature-dependent Ca^{2+} dynamics. As the enzymatic activity in a cell causes local heat pulses, this mechanism may allow cells to operate with high efficiency. In addition, if the correlation between microscopic temperature and highly thermosensitive Ca^{2+} dynamics is fully revealed at the subcellular level, the application of a local heat pulse will become a useful method to manipulate not only tumor cells, such as HeLa, but also other kinds of cells.

MATERIALS AND METHODS

Solutions

The standard medium was 140 mM NaCl, 5 mM KCl, 2 mM $CaCl_2$, 1 mM Na_2HPO_4, 0.5 mM $MgSO_4$, 5 mM glucose, and 10 mM *N*-2-hydroxyethyl piperzine-*N*′-2-ethane sulfonic acid (HEPES) (pH 7.2). We observed the same cellular responses in a solution containing 50 mM HEPES, which means that the phenomena reported here were not caused by the temperature-induced change in the pH buffering ability of extracellular solution. For experiments performed in the absence of extracellular Ca^{2+}, 2 mM ethylene glycol tetra-acetic acid (EGTA) was used instead of 2 mM $CaCl_2$. The intracellular solution (solvent used for injecting fluorescent thermosensitive polymer) was 140 mM KCl, 2 mM $MgCl_2$, 10 mM K_2EGTA, and 10 mM HEPES (pH 7.4). Ca^{2+}-free buffer: 2.7 mM KCl, 137 mM NaCl, 1.5 mM KH_2PO_4, and 8.1 mM Na_2HPO_4. Heparin solution (solvent used for injecting heparin): 30 mg/mL of heparin (low molecular weight) in a pipette dissolved in Ca^{2+}-free buffer.

Microscopy

The optical setup was built around an inverted microscope IX70 (Olympus, Tokyo, Japan) with an objective (UPlanFl, 100×/1.30 Oil, Olympus, Tokyo, Japan) mounted on an optical bench. Both the microheater and the microthermometer were manipulated by three-axis motorized micromanipulators (EMM-3SV, Narishige, Tokyo, Japan). The temperature of the sample (the base temperature) was adjusted by a thermostatically controlled incubator (ONI-INUG2, Tokai Hit, Shizuoka, Japan) placed on the sample stage. A mercury lamp and a filter wheel (Lambda 10-2, Sutter Instrument, Novato, CA, USA) were set outside the bench and connected to the microscope via a liquid light guide, to eliminate the vibration of the sample stage resulting from the rotation of the filter wheel. By using the filter wheel to switch among the excitation filters for europium (III) thenoyltrifluoroacetonate trihydrate (BP360-370, Olympus, Tokyo, Japan), fluorescent thermosensitive polymer (D436/20, Chroma Technology, Rockingham, VT, USA) and Fluo-4 (BP470-490, Olympus, Tokyo, Japan), each fluorophore was imaged. The same dichroic mirror DM505 and the emission filter BA515IF (both from Olympus, Tokyo, Japan) were used for all these fluorophores. (A) For the imaging and analysis of these fluorophores, an electron multiplying charge coupled device (EMCCD) camera (iXon EM+ 897, Andor Technology, Belfast, UK), shooting at 30 frames/s on average, and ANDOR IQ software (Andor Technology, Belfast, UK) were used as the standard setup. (B) Instead of the setup (A), an eight-bit monochrome video rate charge coupled device (CCD) camera (CCD-300, DAGE-MTI, Michigan City, IN, USA) was used for obtaining Fig. 1 and Supplementary Materials, Figs. S1, S2, S3, and S6(D), right, and images were recorded on a digital tape recorder, DSR-45A (Sony, Tokyo, Japan). The recorded images were then digitized by a frame grabber LG3 (Scion Corporation, Frederick, MD, USA) through CREST image [a custom made software modified from National Institutes of Health (NIH) Image by Ryohei Yasuda] with a personal computer (Apple Japan, Tokyo, Japan), and analyzed by ImageJ with a personal computer (Dell, Round Rock, Texas, USA). A Nd:YAG laser (λ=1064 nm, T10-V-106C; 2.5 W, Spectra-Physics, Mountain View, CA, USA) coupled with an optical fiber was also placed outside the bench to avoid vibrations.

Cell culture

HeLa cells were cultured in Dulbecco's modified eagle's medium (DMEM) (Invitrogen, CA, USA) supplemented with fetal bovine serum (10%) and penicillin–streptomycin. Cells were grown in a glass-based dish at 37 °C in the presence of 5% CO_2.

Measurement with fluorescent thermosensitive polymers

Cells were washed and incubated in a standard medium. Then, 2% of poly(DBD-AE-*co*-NNPAM-*co*-NIPAM) (0.1/75/25) dissolved in intracellular solution was loaded in the injection pipette and placed on ice. Just before the injection, the temperature of the dish was decreased to 18 °C. As soon as the injection was completed, the temperature was returned to about 23 °C, where the fluorescence intensity of the polymer started to increase, indicating the beginning of the most sensitive range.

Measurement of $[Ca^{2+}]_{cyt}$ with Fluo-4

Cells were loaded with Fluo-4 by incubation with 1 μM Fluo-4, AM (Invitrogen Corporation, CA, USA) in the standard medium for 45 min at 22±2 °C. Cells were incubated before measurements for 30 min at the desired base temperature. The temperature of the medium had been calibrated in advance by a thermocouple (0.1 °C resolution, Nekken Co., Ltd., Tokyo, Japan).

Image and data analysis

The maximum amplitude of Ca^{2+} overshoot determined by the changes in fluorescence intensity of Fluo-4 (Ca^{2+} indicator), $\Delta F/F_0$, which is shown in Fig. 3(A) and Supplementary Materials, Fig. S6, was determined as $(F_{high}-F_{low})/F_{low}$, where F_{high} is the average of fluorescence intensities for 1 s after it reaches the maximum during Ca^{2+} overshoot, and F_{low} is the average of consecutive three to five data points immediately after heat pulse.

Observation of the convection of the water flow with fluorescent microspheres

Carboxylate-modified yellow–green fluorescent (505/515) microspheres (ϕ=0.2 μm) (Invitrogen, CA, USA) suspension was diluted 20× with distilled water.

SUPPORTING INFORMATION

The following Supplemental Materials accompany this manuscript: Supplementary Materials, Table S1, Supplementary Materials, Fig. S1–S8 with legends, and Supplementary Materials, Videos 1–5 (in the Quick Time format) with legends.

ACKNOWLEDGMENTS

We thank R. DiGiovanni, C. G. dos Remedios and S. V. Mikhailenko for their critical reading of the manuscript. We also thank N. Kurebayashi and T. Kashiyama for helpful discussions. This work was partly supported by Grants-in-Aid for Scientific Research (A), "Academic Frontier" Project, and the 21st Century COE Program (to S.I.) and by Grants-in-Aid for Scientific Research in Priority Areas (to S.I. and M.S.) from the Ministry of Education, Culture, Sports, Science, and Technology of Japan. V. Tseeb and M. Suzuki equally contributed to this work.

REFERENCES

Andersen, P, and Moser, EI (1995). "Brain temperature and hippocampal function." *Hippocampus* **5**, 491–498.

Bahat, A, Tur-Kaspa, I, Gakamsky, A, Giojalas, LC, Breitbart, H, and Eisenbach, M (2003). "Thermotaxis of mammalian sperm cells: a potential navigation mechanism in the female genital tract." *Nat. Med.* **9**, 149–150.

Bennett, DL, Cheek, TR, Berridge, MJ, De Smedt, H, Parys, JB, Missiaen, L, and Bootman, MD (1996). "Expression and function of ryanodine receptors in nonexcitable cells." *J. Biol. Chem.* **271**, 6356–6362.

Berridge, MJ, Bootman, MD, and Lipp, P (1998). "Calcium—a life and death signal." *Nature (London)* **395**, 645–648.

Bers, DM (1989). "SR Ca loading in cardiac muscle preparations based on rapid-cooling contractures." *Am. J. Physiol.* **256**, C109–C120.

Cantor, CR, and Schimmel, PR (1980). *Biophysical Chemistry Part III: The Behavior of Biological Macromolecules*, Freeman, San Francisco, CA.

Dhaka, A, Viswanath, V, and Patapoutian, A (2006). "Trp ion channels and temperature sensation." *Annu. Rev. Neurosci.* **29**, 135–161.

Duhr, S, and Braun, D (2006). "Why molecules move along a temperature gradient." *Proc. Natl. Acad. Sci. U.S.A.* **103**, 19678–19682.

Ehrlich, BE, Kaftan, E, Bezprozvannaya, S, and Bezprozvanny, I (1994). "The pharmacology of intracellular $Ca^{(2+)}$-release channels." *Trends Pharmacol. Sci.* **15**, 145–149.

See EPAPS Document No. E-HJFOA5-3-005902 for supplemental information. For more information on EPAPS, see http://www.aip.org/pubservs/epaps.html.

Hamada, FN, Rosenzweig, M, Kang, K, Pulver, SR, Ghezzi, A, Jegla, TJ, and Garrity, PA (2008). "An internal thermal sensor controlling temperature preference in *Drosophila*." *Nature (London)* **454**, 217–220.

Hamann, HF, O'Boyle, M, Martin, YC, Rooks, M, and Wickramasinghe, HK (2006). "Ultra-high-density phase-change storage and memory." *Nature Mater.* **5**, 383–387.

Hirsch, LR, Stafford, RJ, Bankson, JA, Sershen, SR, Rivera, B, Price, RE, Hazle, JD, Halas, NJ, and West, JL (2003). "Nanoshell-mediated near-infrared thermal therapy of tumors under magnetic resonance guidance." *Proc. Natl. Acad. Sci. U.S.A.* **100**, 13549–13554.

Inoue, T, and Nakaoka, Y (1990). "Cold-sensitive responses in the paramecium membrane." *Cell Struct. Funct* **15**, 107–112.

Kam, NWS, O'Connell, M, Wisdom, JA, and Dai, H (2005). "Carbon nanotubes as multifunctional biological transporters and near-infrared agents for selective cancer cell destruction." *Proc. Natl. Acad. Sci. U.S.A.* **102**, 11600–11605.

Kato, H, Nishizaka, T, Iga, T, Kinosita, K, Jr., and Ishiwata, S (1999). "Imaging of thermal activation of actomyosin motors." *Proc. Natl. Acad. Sci. U.S.A.* **96**, 9602–9606.

Kondepudi, D, and Prigogine, I (1998). *Modern Thermodynamics*, Wiley, Chichester, West Sussex, UK.

Maeda, K, Imae, Y, Shioi, JI, and Oosawa, F (1976). "Effect of temperature on motility and chemotaxis of *Escherichia coli*."*J. Bacteriol.* **127**, 1039–1046.

Meissner, G (1986). "Ryanodine activation and inhibition of the Ca^{2+} release channel of sarcoplasmic reticulum." *J. Biol. Chem.* **261**, 6300–6306.

Mikoshiba, K (2007). "IP_3 receptor/Ca^{2+} channel: from discovery to new signaling concepts." *J. Neurochem.* **102**, 1426–1446.

Paster, E, and Ryu, WS (2008). "The thermal impulse response of *Escherichia coli*." *Proc. Natl. Acad. Sci. U.S.A.* **105**, 5373–5377.

Patapoutian, A, Peier, AM, Story, GM, and Viswanath, V (2003). "ThermoTRP channels and beyond: mechanisms of temperature sensation." *Nat. Rev. Neurosci.* **4**, 529–539.

Pissuwan, D, Valenzuela, SM, and Cortie, MB (2006). "Therapeutic possibilities of plasmonically heated gold nanoparticles." *Trends Biotechnol.* **24**, 62–67.

Plieth, C, Hansen, UP, Knight, H, and Knight, MR (1999). "Temperature sensing by plants: the primary characteristics of signal perception and calcium response." *Plant J.* **18**, 491–497.

Protasi, F, Shtifman, A, Julian, FJ, and Allen, PD (2004). "All three ryanodine receptor isoforms generate rapid cooling responses in muscle cells." *Am. J. Physiol.: Cell Physiol.* **286**, C662–C670.

Sakai, T (1986). "Rapid cooling contracture." *Jpn. J. Physiol.* **36**, 423–431.

Sitsapesan, R, Montgomery, RAP, MacLeod, KT, and Williams, AJ (1991). "Sheep cardiac sarcoplasmic reticulum calcium-release channels: modification of conductance and gating by temperature." *J. Physiol. (London)* **434**, 469–488.

Sung, DY, Kaplan, F, Lee, KJ, and Guy, CL (2003). "Acquired tolerance to temperature extremes." *Trends Plant Sci.* **8**, 179–187.

Talon, S, Huchet-Cadiou, C, and Leoty, C (2000). "Rapid cooling-induced contractures in rat skinned skeletal muscle fibres originate from sarcoplasmic reticulum Ca^{2+} release through ryanodine and inositol trisphosphate receptors." *Pfluegers Arch.* **441**, 108–117.

Uchiyama, S, Matsumura, Y, de Silva, AP, and Iwai, K (2004). "Modulation of the sensitive temperature range of fluorescent molecular thermometers based on thermoresponsive polymers." *Anal. Chem.* **76**, 1793–1798.

Warner, DA, and Shine, R (2008). "The adaptive significance of temperature-dependent sex determination in a reptile." *Nature (London)* **451**, 566–568.

Zeeb, V, Suzuki, M, and Ishiwata, S (2004). "A novel method of thermal activation and temperature measurement in the microscopic region around single living cells." *J. Neurosci. Methods* **139**, 69–77.